



HAL
open science

First EISCAT measurement of electron-gas temperature in the artificially heated D-region ionosphere

A. Kero, T. Bösinger, P. Pollari, E. Turunen, M. Rietveld

► **To cite this version:**

A. Kero, T. Bösinger, P. Pollari, E. Turunen, M. Rietveld. First EISCAT measurement of electron-gas temperature in the artificially heated D-region ionosphere. *Annales Geophysicae*, 2000, 18 (9), pp.1210-1215. hal-00316792

HAL Id: hal-00316792

<https://hal.science/hal-00316792>

Submitted on 18 Jun 2008

HAL is a multi-disciplinary open access archive for the deposit and dissemination of scientific research documents, whether they are published or not. The documents may come from teaching and research institutions in France or abroad, or from public or private research centers.

L'archive ouverte pluridisciplinaire **HAL**, est destinée au dépôt et à la diffusion de documents scientifiques de niveau recherche, publiés ou non, émanant des établissements d'enseignement et de recherche français ou étrangers, des laboratoires publics ou privés.

First EISCAT measurement of electron-gas temperature in the artificially heated D-region ionosphere

A. Kero¹, T. Bösinger¹, P. Pollari¹, E. Turunen², M. Rietveld³

¹ University of Oulu, Department of Physical Sciences, FIN-90401 Oulu, Finland

² Geophysical Observatory, FIN-9960 Sodankylä, Finland

³ EISCAT, 9027 Ramfjordbotn, Norway; also at Max-Planck-Institut für Aeronomie, D-37191 Katlenburg-Lindau, Germany

Received: 14 February 2000 / Revised: 14 June 2000 / Accepted: 15 June 2000

Abstract. The ionospheric electron gas can be heated artificially by a powerful radio wave. According to our modeling, the maximum effect of this heating occurs in the D-region where the electron temperature can increase by a factor of ten. Ionospheric plasma parameters such as N_e , T_e and T_i are measured by EISCAT incoherent scatter radar on a routine basis. However, in the D-region the incoherent scatter echo is very weak because of the low electron density. Moreover, the incoherent scatter spectrum from the D-region is of Lorentzian shape which gives less information than the spectrum from the E- and F-regions. These make EISCAT measurements in the D-region difficult. A combined EISCAT VHF-radar and heating experiment was carried out in November 1998 with the aim to measure the electron temperature increase due to heating. In the experiment the heater was switched on/off at 5 minute intervals and the integration time of the radar was chosen synchronously with the heating cycle. A systematic difference in the measured autocorrelation functions was found between heated and unheated periods.

Key words: Ionosphere (active experiments; plasma temperature and density; wave propagation)

1 Introduction

At first glance it looks surprising that there are – to our knowledge – no reports on EISCAT measurements devoted to one of the most dramatic effects of “heating experiments”, the heating of the electron gas in the D-region ionosphere. There was an EISCAT experiment back in 1985 (E. Turunen in EISCAT Annu Rep 1985, EISCAT Sci Assoc, Kiruna, 1985) where this issue was

addressed in passing. This experiment was, however, designed and carried out for a different purpose.

It also looks surprising from a general point of view, that the electron temperature belongs to the ionospheric parameters readily derived by routine EISCAT measurements, such as the CP (common program) measurements, at least above 90 km, and it is often referred to as the uniqueness of the HF heating facility at Tromsø that an incoherent scatter radar, EISCAT, is operating in parallel to the device, just at the same spot. There were several attempts at doing D-region electron-temperature measurements in the early 1990s but without success. Quite in contrast, there are in fact many reports on strong heating of electron gas in the F-region (Robinson *et al.*, 1996; Honary *et al.*, 1993; Stocker *et al.*, 1992; Jones *et al.*, 1986). Reasons why the heating-induced electron temperature enhancement at D-region heights has not yet been measured may be: (1) too short an integration time; (2) wrong conditions or time of day; (3) non-optimum HF parameters (see our discussion). The negative outcome so far is still a surprise, since the heating-induced electron temperature enhancements always exhibit a maximum in D-region heights, and this maximum can be quite substantial (up to a factor of ten) and may often be associated with the largest wave-energy absorption. Here we report our first successful attempt at doing this measurement.

The heating effect is caused by collisions between neutral particles and electrons accelerated by the radio wave. The D-region is an ideal place for this wave-electron-neutral interaction because of already sufficient electron density N_e and still high collision frequency ν_{en} between electrons and neutrals. In these collisions a part of the energy of the radio wave is transferred to thermal energy of electrons. By this absorption the wave is, of course, diminished and thereby the heating effect is usually weakened above the D-region. Below the D-region the collision frequency is too high for the wave to accelerate electrons between the collisions. Unfortunately the D-region is also the most difficult target for the incoherent scatter radar technique because of low electron density, high collision frequency and

Correspondence to: A. Kero
e-mail: akero@mail.student.oulu.fi

exotic ion chemistry. Therefore, artificial heating is not used to a great extent in D-region studies and in most cases scientists try to investigate effects in the E- or F-regions. This is done by choosing the radio wave parameters (frequency, radiative power and polarization) so as to minimize the interaction between the wave and the electrons for the D-region. In our case, the parameters were chosen with the opposite intention.

2 Description of the experiment

The EISCAT heating facility provides various methods for carrying out heating experiments (Rietveld *et al.*, 1993). Basically, the user must choose the antenna field (out of three arrays), frequency and polarization of the radio wave and various modulation schemes of these parameters during the heating. In our experiment, the largest antenna field (array 1) was used to produce as narrow a beam as possible and thereby the maximum radiated power in the heated area. All 12 transmitters were used with 75 kW each. Antenna array 1 has a gain of 30 dB at the chosen frequency of 5.423 MHz so that the *effective radiative power*, ERP¹ was 900 MW. The polarization (X-mode) and the frequency of the wave were chosen to create the main effect somewhere between 70 and 80 km altitudes. This was estimated by our theoretical heating model described in section 3.

The experiment was started on 19 November 1998, at 20.30 UT and lasted three and a half hours. In order to see the difference between heated and unheated plasma, the heater was switched on/off every 5 minutes. The EISCAT VHF-radar (224 MHz) was looking at the same region in the sky with a special D-region program GEN-11 (Turunen, 1986). The post-integration time of the radar was chosen synchronously with the heating cycle.

3 Theoretical heating model

As mentioned already the experiment was designed by using our own heating model. The approach is very much the same as in Belova *et al.* (1995).

3.1 Absorption of the radio wave

Radio wave propagation in the ionospheric D-region is described by the well known Appleton-Lassen dispersion relation

$$n^2 = 1 - \frac{X}{1 - iZ - \frac{(Y \sin \theta)^2}{2(1-X-iZ)} \pm \sqrt{\frac{(Y \sin \theta)^4}{4(1-X-iZ)^2} + (Y \cos \theta)^2}}, \quad (1)$$

¹ ERP is the power from an isotropically radiating antenna which would give the same power density as that in the main lobe of the actual antenna beam. The heater beam of the antenna array 1 is about 7° wide and for that ERP ~ 900 MW.

which describes the refractive index n of the plasma as a function of normalized frequencies X, Y, Z , defined as

$$X = \frac{\omega_{pe}^2}{\omega^2} = \frac{N_e e^2}{\epsilon_0 m_e \omega^2}, \quad (2)$$

$$Y = \frac{\omega_{ge}}{\omega} = \frac{eB}{m_e \omega} \quad (3)$$

and

$$Z = \frac{v_{en}}{\omega}. \quad (4)$$

Symbols $e, \epsilon_0, m_e, \omega$ and B stand for unit charge, permittivity of vacuum, mass of electron, angular frequency of the radio wave and external magnetic field respectively. The angle between the wave vector and the direction of the magnetic field is denoted by the symbol θ . The B -field is the magnetic field of the Earth that is obtained within a dipole field approximation. The electron-neutral collision frequency v_{en} is calculated from Dalgarno *et al.*, (1967)

$$v_{en} = 1.7 \times 10^{-11} [N_2] T_e + 3.8 \times 10^{-10} [O_2] \sqrt{T_e} + 1.4 \times 10^{-10} [O] \sqrt{T_e}, \quad (5)$$

where neutral densities (constituents with square brackets) and the electron temperature must be given in units cm^{-3} and Kelvin. It can be shown that the refractive index is a complex number with a negative imaginary part $\text{Im}(n) < 0$ when electron-neutral collisions are involved in the plasma ($Z > 0$), so the imaginary part of n describes the damping of the wave. The physical interpretation of the damping is that part of the wave energy is absorbed into the plasma. This energy is actually divided between electrons and neutrals but because of the huge mass difference the electrons take practically all of it. By using an ideal gas approximation for the electron gas, the electron temperature variation due to the absorption is described by the non-linear differential equation

$$\frac{dT_e}{dt} = \frac{2}{3k_B N_e} \left(-\text{Im}(n) \frac{2\omega I}{c} - L \right), \quad (6)$$

where I is the intensity of the wave and L is the sum of all electron energy loss-functions (Stubbe and Varnum, 1972; Prasad and Furman, 1973). When this equation is solved numerically for D-region conditions, it turns out that the electron temperature achieves an equilibrium $dT_e/dt = 0$ on tens of microseconds timescale. The rapid response of the plasma is due to the high collision frequency v_{en} and it is experimentally verified when heating is used to produce artificial magnetic disturbances (Rietveld *et al.*, 1986). The electron temperature is thereby considered to achieve its maximum immediately when the heater is switched on, and it stays constant until the heater is switched off.

3.2 Algorithm

The equilibrium state can be determined by solving numerically Eq. (6) as a function of T_e with initial

condition $dT_e/dt = 0$. The parameters for this calculation from Eqs. (1)–(6) are $\theta, \omega, N_e, B, [N_2], [O_2], [O]$ and T_n . In our model the electron density profile is given by the Sodankylä Ion Chemistry SIC model (Turunen *et al.*, 1996) and the neutral atmosphere parameters are taken from MSISE90-model (Hedin, 1991).

The intensity of the wave I must be calculated for each altitude (see Eq. 6) by taking into account the absorption below. Using the ERP, the intensity at height h is given by

$$I = \frac{ERP}{4\pi h^2} \exp\left(\int_0^h \frac{2\omega}{c} \text{Im}(n) dh\right). \quad (7)$$

In practice, the integral is approximated by a sum over 1 km layers below the altitude h . After calculating the intensity and solving the T_e in equilibrium, the model goes on to the next layer.

By introducing the input parameters corresponding to our experiment on 19 November 1998, the model gives the electron temperature profile in the heated D-region as shown in Fig. 1). The maximum heating effect appears to be somewhere around 75 km and there is a strong decay above it. This can be understood in the way that practically all of the wave is absorbed in the D-region. It turns out that a similar decrease of the heating effect showed up in the data of the EISCAT GEN-11 experiment. This indicates that our absorption estimates are realistic as compared to the actually occurring heating effect.

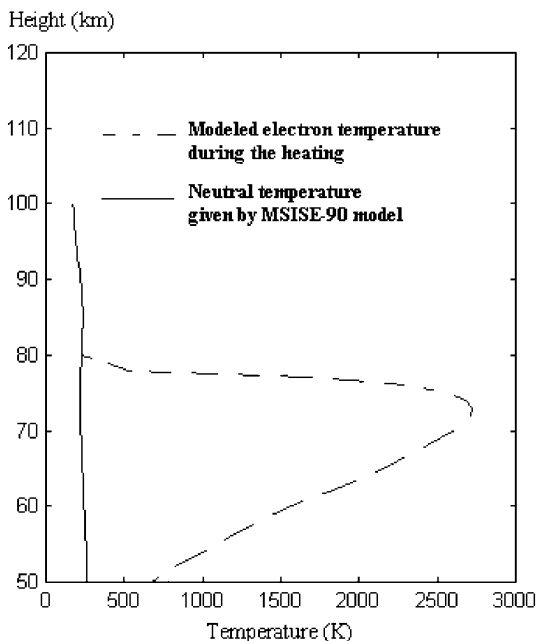


Fig. 1. Our modeled electron temperature (*dashed line*) and MSISE-90 model neutral temperature (*solid line*) as a function of height. The MSISE-90 inputs are adopted according to the situation at the heating experiment on 19 November 1998

4 The data and the analysis of it

The incoherent scatter radar measurement output is first a set of autocorrelation functions (ACF). For the GEN-11 experiment the ACF is measured for 42 gates corresponding to altitudes from 70 to 113 km in 1.05 km steps. Each ACF contains 22 values in the time domain. The shortest time lag is 112 μ s (later called lag0) and the longer lags (lag1 – lag21) come in multiples of 3.24 ms. The measured ACFs are the product of the *autocorrelation function of the target plasma* and the radar *ambiguity function*. The latter contains the effect of the receiver impulse response and the transmitter modulation. The purpose is to separate the measurement device effects (ambiguity function) from the pure ACF of the plasma. This ambiguity correction is done here with the method described in Pollari *et al.* (1989). Practically, the correction is significant only for the lag0+ and lag1 values.

4.1 Measured autocorrelation functions

Ambiguity corrected data points are shown in Fig. 2. The results shown here are the averages over the whole experiment so that each crossed ball represents the average of all 21 heating-on periods and the open balls heating-off periods. Note that the ACFs in the lower gates are rather noisy and thereby the post-integration over long timescales is unavoidable in our data analysis.

One can see a systematic difference between the ACFs measured during heated as compared to unheated time periods. In the heated periods the average ACFs are decaying more rapidly as a function of lag, and the absolute values of the first lags are smaller as compared to the unheated ones. Note also, that the difference is reduced in higher gates, which is in agreement with the predicted decrease of the heating influence above the maximum altitude (see Fig. 1).

4.2 Data analysis

Plasma parameters ($N_e, T_e/T_i, v_i$, etc.) are obtained by fitting a theoretical ACF to the measurement points, so that some parameters are used as free variables and the rest of the quantities are assumed to be constant. This fitting can be done automatically with GUIDAP for most of the EISCAT experiments. Unfortunately, GUIDAP cannot handle pulse-to-pulse correlation programs such as GEN-11 by its very design. The method used in this paper should be considered as a preliminary data-analysis approach. More work has to be done to reach routine data analysis of the given type.

The theoretical plasma ACF is inverse Fourier transform of the power spectral density function. The full formulation of the power spectrum is given by Dougherty and Farley (1963) and several approximations are also used in some special cases. In the D-region ionosphere the incoherent scatter spectrum can be assumed to be of Lorentzian shape and the corresponding

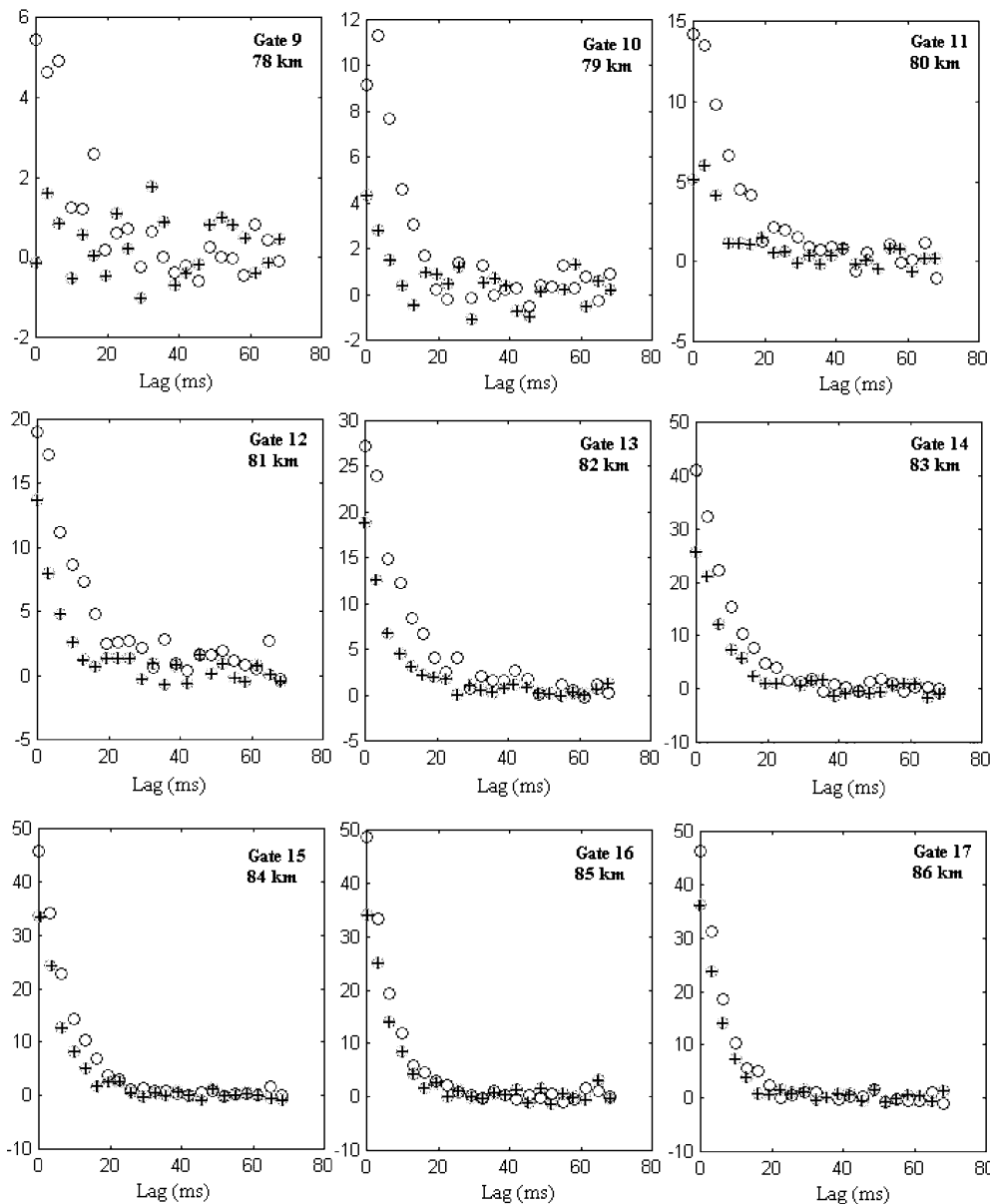


Fig. 2. Measured average, ambiguity corrected, autocorrelation functions for gates 9–17. Each of the balls represents the average over 21 heating-on (*crossed balls*) or heating-off (*open balls*) periods

ACF is thereby exponential. By taking into account the effect of negative ions (Fukuyama and Kofman, 1980), the actual electron density and the temperature of the plasma can successfully be obtained by this approach. The approximation of the exponential ACF is often used in the GEN-11 data analysis. However, in the following fitting, the ACF is obtained by using the full spectrum form. Hence, one can be sure that the dependence of the ACF shape on the electron temperature is correct in circumstances of the heated ionosphere, where $T_e \gg T_i$.

The incoherent scatter spectrum is a function of all plasma constituents. This is a challenge for the spectrum model especially in the D-region where the ion chemistry is very complex. Here the calculation of the power spectral density function is based on the SIC-model so that concentration of all 33 positive and 18 negative ion species to the spectrum are taken into account. Theoretical ACF is calculated by using the inverse fast

Fourier transform (IFFT) algorithm to the power spectral density function. Electron temperature estimates are obtained by using T_e as a free parameter in fitting the theoretical ACF to the measured one in a least squares fashion. In order to scale the measured and the theoretical ACFs in a similar way, the measurement points are normalized so that all of the lag values are divided by the unheated lag1 value. The theoretical curve is normalized correspondingly, so that the ACF (for every T_e/T_i -ratio) is divided by the ACF value at point 3.24 ms (=lag1) in the $T_e = T_i$ condition. The value of lag1 was chosen to be the normalization point, instead of lag0, because lag1 is less noisy.

5 Discussion

The best-fitting ACFs (gates 9, 11 and 17) are shown in Fig. 3). One can see that the theoretical ACFs can

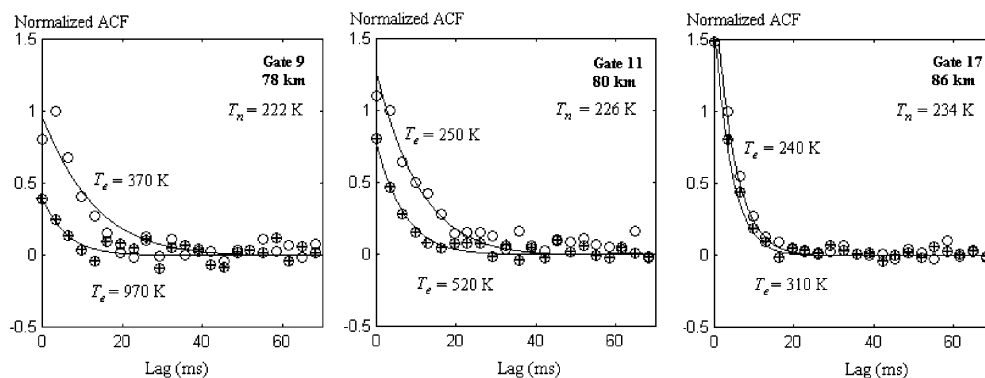


Fig. 3. Best fittings of the theoretical plasma ACFs (*solid line*) to the ambiguity corrected data points (*balls*) for the gates 9, 11 and 17. The *crossed* and *open* balls stand for the heating-on and heating-off periods, respectively. The neutral temperature was taken from the MSISE-90 model, and the ion temperature was assumed to be equal to the neutral temperature

successfully be fitted to the averaged measurement points as a function of T_e . Though the fitting in gate 9 seems to be imperfect, especially in the unheated case, a rough estimation of the average electron temperatures can nevertheless be obtained also in that altitude. One possible error source in the fitting is the electron density, which is not obtained from the analysis, but taken directly from the SIC-model. However, the average heated electron temperature measured by EISCAT and analyzed based on the SIC-model seems to be reasonably well in agreement with the theoretical radio wave absorption calculation (see Fig. 4). The main heating effect appears to be somewhere below the best altitude range for the EISCAT GEN-11 type experiment. Nevertheless, the predicted decay of the effect due to the strong absorption is clearly visible in the measured data. The original aim was naturally to measure the maximum effect, but this time the radio wave parameters were such that the absorption turned out to be at too low D-region altitudes. The design of the heating experiment is difficult mainly due to variable electron density, which should be known in advance. The SIC-model gives a very detailed view of the D-region and it

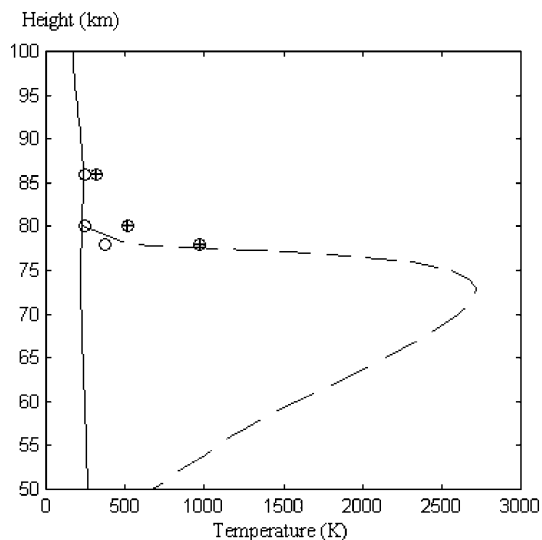


Fig. 4. The measured average electron temperatures during heating-on (*crossed balls*) and heating-off (*open balls*) periods in comparison to the modeled heating effect (*dashed line*). The neutral temperature profile (*solid line*) is taken from MSISE-90 model

seems to be a usable tool, not only for predicting the electron density profile, but also for calculating the realistic incoherent scatter spectrum for the D-region.

Note that our results reflect in the best case a time average over an hour or so of the heating effect. No doubt, especially during sun rise, sun set or particle precipitation events, the D-region parameters may change on a much shorter timescale affecting the efficiency of the heating in a direct way. This experiment was meant to demonstrate that the heating effect can indeed be measured. By optimizing our tools and methods we are confident that in the near future we will also be able to demonstrate the variability in the heating efficiency in accord to changing ionospheric conditions.

6 Conclusions

By our experiment we have succeeded to demonstrate that it is in fact possible to measure by EISCAT the heating-induced electron temperature increase in the D-region, in spite of the fact that our experiment design and the geophysical conditions were not fully optimal for our purpose. With the experience gained by this experiment there are good reasons to believe that it will be possible in the near future to carry out still more accurate measurements of this kind. The D-region is geophysically a very interesting and in many respects an important layer where the collision-dominated neutral atmosphere and the plasma-dominated ionosphere intersect. Moreover, the D-region has an exotic ion chemistry including negative ions.

Newly designed EISCAT measurements and more extensive data-analysis including different local times and geophysical conditions will make it possible, especially in application with heating, to verify and improve existing D-region models. After such long operation of EISCAT and the Tromsø HF heating facility it was a surprise for us that the missing link of D-region electron temperature measurement in conjunction with heating could finally be found with relative ease.

Acknowledgements. We are indebted to the director and staff of EISCAT for operating the radar and heating facilities and greatly acknowledge the support of all the individuals and personnel of the institutions who contributed to the Finnish EISCAT heating experiment. EISCAT is an international association supported by

Finland (SA), France (CNRS), the Federal Republic of Germany (MPG), Japan (NIPR), Norway (NFR), Sweden (NFR) and the United Kingdom (PPARC). The author and student A.K. acknowledges financial support by the Academy of Finland.

Topical Editor M. Lester thanks J. Silen and another referee for their help in evaluating this paper.

References

- Belova, E. G., A. B. Pashin, and W. B. Lyatsky**, Passage of a powerful HF radio wave through the lower ionosphere as a function of initial electron density profiles, *J. Atmos. Terr. Phys.*, **57**, 265–272, 1995.
- Dalgarno, A., M. B. McElroy, and J. C. G. Walker**, The diurnal variation of ionospheric temperatures, *Planet. Space Sci.*, **15**, 331–345, 1967.
- Dougherty, J. P., and D. T. Farley**, A theory of incoherent scattering of radio waves by a plasma, *J. Geophys. Res.*, **68**, 5473–5486, 1963.
- Fukuyama, K., and W. Kofman**, Incoherent scattering of an electromagnetic wave in the mesosphere: a theoretical consideration, *J. Geomagn. Geoelectr. Kyoto*, **32**, 67–81, 1980.
- Hedin, A. E.**, Extension of the MSIS Thermosphere model into the middle and lower atmosphere, *J. Geophys. Res.*, **96**, 1159–1172, 1991.
- Honary, F., A. J. Stocker, T. R. Robinson, T. B. Jones, N. M. Wade, P. Stubbe, and H. Kopka**, EISCAT observations of electron temperature oscillations due to the action of high power HF radio waves, *J. Atmos. Terr. Phys.*, **55**, 1433–1448, 1993.
- Jones, T. B., T. R. Robinson, P. Stubbe, and H. Kopka**, EISCAT observations of the heated ionosphere, *J. Atmos. Terr. Phys.*, **48**, 1027–1035, 1986.
- Pollari, P., A. Huuskonen, E. Turunen, and T. Turunen**, Range ambiguity effects in a phase coded D-region incoherent scatter radar experiment, *J. Atmos. Terr. Phys.*, **51**, 937–945, 1989.
- Prasad, S. S., and D. R. Furman**, Electron energy transfer rates in the ionosphere, *J. Geophys. Res.*, **78**, 6701–6707, 1973.
- Rietveld, M. T., H. Kopka, and P. Stubbe**, D-region characteristics deduced from pulsed ionospheric heating under auroral electrojet conditions, *J. Atmos. Terr. Phys.*, **45**, 311–326, 1986.
- Rietveld, M. T., H. Kohl, H. Kopka, and P. Stubbe**, Introduction to ionospheric heating at Tromsø, I. Experimental overview, *J. Atmos. Terr. Phys.*, **55**, 577–599, 1993.
- Robinson, T. R., F. Honary, A. J. Stocker, T. B. Jones, and P. Stubbe**, First EISCAT observations of the modification of F-region electron temperatures during RF heating at harmonics of the electron gyrofrequency, *J. Atmos. Terr. Phys.*, **58**, 385–395, 1996.
- Stocker, A. J., F. Honary, T. R. Robinson, T. B. Jones, P. Stubbe, and H. Kopka**, EISCAT observations of large scale electron temperature and electron density perturbations caused by high power HF radio wave, *J. Atmos. Terr. Phys.*, **54**, 1555–1572, 1992.
- Stubbe, P., and W. S. Varnum**, Electron energy transfer rates in the ionosphere, *Planet. Space Sci.*, **20**, 1121–1126, 1972.
- Turunen, T.**, GEN-SYSTEM – a new experimental philosophy for EISCAT radars, *J. Atmos. Terr. Phys.*, **48**, 777–785, 1986.
- Turunen, E., H. Matveinen, J. Tolvanen, and H. Ranta**, D-region ion chemistry model. In *Solar terrestrial energy program: SCOSTEP handbook of ionospheric models*, Ed. R. W. Schunck, 1–25, 1996.